Analysis of uncertainties in the prediction of ships' fuel consumption – from early design to operation conditions

Citation for the original published paper (version of record):
Tillig, F., Ringsberg, J., Mao, W. et al (2018). Analysis of uncertainties in the prediction of ships' fuel consumption – from early design to
operation conditions. Ships and Offshore Structures, 13: 13-24.
http://dx.doi.org/10.1080/17445302.2018.1425519

SHIPS AND OFFSHORE STRUCTURES
2018, VOL. 13, NO. S1, S13– S24
https://doi.org/10.1080/17445302.2018.1425519

Taylor & Francis
Taylor & Francis Group

Analysis of uncertainties in the prediction of ships' fuel consumption – from early design to operation conditions

Fabian Tillig, Jonas W. Ringsberg, Wengang Mao and Bengt Ramne

Division of Marine Technology, Department of Mechanics and Maritime Sciences, Chalmers University of Technology, Gothenburg, Sweden

ABSTRACT

This investigation presents an approach towards a better understanding of achievable accuracy of fuel consumption predictions of ships and provides an example of how a thorough uncertainty analysis of prediction models can be performed. A generic ship energy systems model is used for the fuel consumption prediction of two reference ships: a RoRo ship and a tanker. The study presents how uncertainties can be categorised and handled in four different phases of a ship's life – from early design to ship operation. Monte Carlo simulations are carried out for two environmental conditions to calculate the mean and uncertainty of the fuel consumption. The results show that the uncertainty in the fuel consumption prediction in a very early phase of the design process is approximately 12%, whereas at a very late phase, it reduces to less than 4%. Finally, the simulation model is applied to a real ship during operation conditions.

ARTICLE HISTORY
Received 4 October 2017
Accepted 4 January 2018

KEYWORDS
Fuel consumption; Monte Carlo simulation; ship design; ship energy efficiency; ship operation; uncertainty analysis

Nomenclature

A_L	Longitudinal area above the waterline (m^2)
A_T	Transversal area above the waterline (m^2)
B	Beam (m)
B_h	Superstructure beam (m)
c_B	Block coefficient
c_F	Frictional resistance coefficient
CFD	Computational fluid dynamics
c_R	Residual resistance coefficient
c_X	Wind resistance coefficient
D_h	Depth (m)
FC	Fuel consumption (t/nm, t/h)
Fn	Froude number
h	Superstructure height (m)
J	Propeller advance ratio
k	Form factor
K_T	Thrust coefficient (propeller)
K_Q	Torque coefficient (propeller)
L_h	Superstructure length (m)
L_{oa}	Length over all (m)
L_{PP}	Length between perpendiculars (m)
P/D	Propeller pitch-to-diameter ratio
R_{AW}	Added resistance due to waves (N)
$SFOC$	Specific fuel consumption (kg/kWh)
SL	Slenderness ratio ($L_{pp}/\sqrt[3]{\nabla}$)
S_W	Wetted surface (m^2)
t	Thrust deduction
T_m	Mean draft (m)
v_{AW}	Apparent wind speed (kn, m/s)
v_S	Ship speed (kn, m/s)
w_e	Effective wake
η_H	Hull efficiency
η_0	Propeller open water efficiency
ρ_{Air}	Air density (1.25 kg/m^3)
ρ_{SW}	Sea water density (1025 kg/m^3)

1. Introduction

To improve the energy efficiency of ships, we must be able to accurately predict and analyse the performance of ships not only during operation but also during the design of new ships. A practical and useful prediction method for such purposes should be applicable both without prior measurements and for an arbitrary ship; additionally, the expected accuracy of the prediction must be quantified.

In recent years, simulation models to predict and analyse the complex system 'ship' in operational conditions were introduced, for example by Leifsson et al. (2008), Vinther-Hansen (2011), Calleya et al. (2015), Lu et al. (2015), Cichowicz et al. (2015) and Tillig et al. (2017). All of the mentioned simulation models require different amounts of information and levels of detail; thus, some are more suitable for prediction in the early ship design phase, and others are better for the performance analysis of ships in service. The models presented by Calleya et al. (2015), Cichowicz et al. (2015) and Tillig et al. (2017) are capable of predicting the fuel consumption (FC) during the design or the impact of retrofitting projects on the operational performance, while the other models are focused on the operational performance analyses of existing ships and require more detailed input or even full-scale measurements. A more detailed review of existing performance prediction models can be found in Tillig et al. (2017).

With different prediction methods at hand, the shipping industry still lacks a quantification of the 'expected prediction accuracy' and an understanding of the possibilities for increasing the accuracy. In the present study, a further developed ver-

CONTACT Fabian Tillig tillig@chalmers.se

sion of the ship energy systems model presented by Tillig et al. (2017) is used to analyse the achievable accuracy of FC predictions in different phases of a ship's life – from early design to ship operation.

1.1. Uncertainties in the prediction of the fuel consumption

The categorisation and quantification of uncertainties is performed using the simulation model presented in Tillig et al. (2017). The accuracy of a prediction depends on, among other factors, the amount of information that is available at each phase together with the methods used. Equation (1) presents an expression for the FC and exemplifies the complexity and coupling between several factors (with the identified random variables printed in bold):

$$FC = \boldsymbol{SFOC} * \left(\boldsymbol{S_W} * (c_F + (\boldsymbol{k} * \boldsymbol{c_F} + \boldsymbol{c_R})) * \frac{\rho_{SW}}{2} * v_S^2 + \boldsymbol{c_X} * \boldsymbol{A_T} * \frac{\rho_{Air}}{2} * v_{AW}^2 + \boldsymbol{R_{AW}} \right) / \boldsymbol{\eta_0} / \boldsymbol{n_h} * v_S. \quad (1)$$

Uncertainties can be classified into aleatoric and epistemic. The aleatoric uncertainty is known as statistical uncertainty which is representative for unknowns that differ each time we make a measurement, e.g. the sea state condition. The epistemic uncertainty is a systematic uncertainty that is associated with imperfect models of the real world. According to Kennedy and O'Hagan (2001), there are several sources of uncertainties:

(1) Parametric variability comes from the variability of input variables of the model. For example, the manufactured hull shape may differ from the designed hull.
(2) Parameter uncertainty comes from the model parameters that are input into the mathematical model. Their exact values are often unknown and cannot be exactly represented by statistical methods.
(3) Structural uncertainty (i.e. model inadequacy) is the lack of knowledge of the underlying true physics.
(4) Experimental uncertainty (observation error) is the variability of experimental measurements.
(5) Interpolation uncertainty is the lack of available data collected from computer model simulations and/or experimental measurements.

Table 1. Dimensional ratios of the two reference ships.

Dimensional ratios	RoRo ship	Tanker
L_{pp}/B	6.87	5.42
B/T	3.47	2.93
c_B	0.69	0.79
SL ($L_{pp}/\sqrt[3]{\nabla}$)	6.19	4.78
Fn (design/operation)	0.23/0.19	0.16

(6) Algorithmic uncertainty (numerical uncertainty) is related to numerical errors and approximations from the computer model.

In this investigation, 'Design uncertainty' is used as the term for source 1, parametric variability. The uncertainty that refers to sources 2–5 is referred to as 'Method uncertainty'. Source 6, algorithmic uncertainty, is not studied explicitly.

Two reference ships are studied under two environmental conditions: calm water and no wind, as well as head waves (sea state 4) and Beaufort 4 headwind. The former represents the traditional contract condition, and the latter represents a real-life operational condition.

Table 1 presents an overview of the principal dimensional ratios of the reference ships. Calm water model tests and hull forms were available for both ships.

The analyses are divided into four design phases, which are important milestones in the design process: (I) Concept design where only the main dimensions are known; (II) Finished hull and propeller design; (III) Completed calm water model tests; and (IV) Finished ship design (i.e. including the superstructure). Table 1 presents an overview of the design and method uncertainties related to the terms of Equation (1). It includes the relevant design phase and section of the study in which they are evaluated and discussed. A detailed description of each variable and its uncertainty (values shown in brackets), is given in Table 2.

2. A generic ship energy systems model

The ship energy systems model presented in Tillig et al. (2017) is used for the power prediction in the investigation. Generally, the model follows the ITTC78 (ITTC 1999) approach concerning resistance and propulsive coefficients. A flowchart of the model is presented in Figure 1.

In Tillig et al. (2017), the model and its components are described in detail. Below, a brief introduction is given for each component as numbered in the flowchart in Figure 1.

Table 2. The design (D) and method (M) uncertainties in the simulation model at different design phases.

	Design phase			
Variable	I	II	III	IV
Wetted surface (S_w)	D (5.1)	–	–	–
Calm water resistance coefficients ($k * c_F + c_R$)	M (4.2), D (5.2)	M (4.2)	M (4.2)	M (4.2)
Effective wake (w_e)	M (4.3), D (5.3)	M (4.3)	M (4.3)	M (4.3)
Hull efficiency (η_h)	M (4.4)	M (4.4)	M (4.4)	M (4.4)
Air/wind resistance (c_X, A_T, A_L)	M (4.9), D (5.5)	M (4.9), D (5.5)	M (4.9), D (5.5)	M (4.9)
Propeller efficiency (η_0)	M (4.5), D (5.4)	M (4.5)	M (4.5)	M (4.5)
Added resistance in waves (R_{AW})	M (4.6), D (5.6)	M (4.6)	M (4.6)	M (4.6)
Main engine $SFOC$	M (4.7)	M (4.7)	M (4.7)	M (4.7)

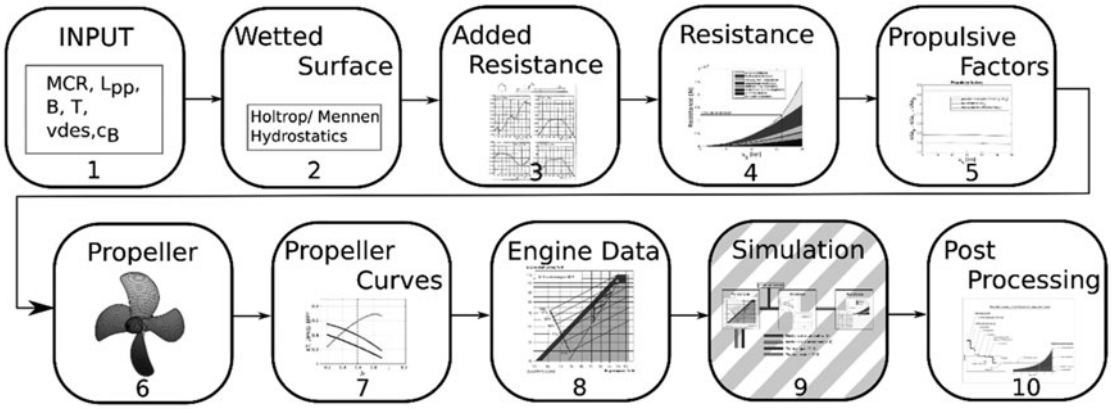

Figure 1. Flowchart of the generic energy systems model.

(1) The generic energy systems model is set up to be usable with very limited input. Only the main dimensions (length, beam, draft, displacement), the propeller rpm and the ship and engine type are needed for a power prediction.
(2) The wetted surface is based on a numerical hull standard series, which is further described below.
(3) Added resistance due to wind and waves are included in the model as described as follows.
   (a) The wind resistance coefficients are taken from Blendermann (1994) and windage areas are estimated based on the ship size and type.
   (b) The added wave resistance is estimated using the average of three different methods: the STA2 method (ITTC 2014b), the method developed in Liu and Papanikolaou (2016) (NTUA-SDL) and a modified version of the NTUA-SDL method (Liu et al. (2016)).
(4) The calm water resistance is computed using the average of three different methods: (i) the method developed in Kristensen and Lützen (2012), (ii) the method developed by Hollenbach (Hollenbach 1998), and (iii) results from full-scale computational fluid dynamics (CFD) computations using the hull form from the numerical standard series.
(5) The effective wake is estimated using the average of the methods by Schneekluth, Krüger, Heckscher, and Troost (Bertram and Schneekluth 1998) and Harvald (Kristensen and Lützen 2012). Due to the difficulties in predicting the thrust deduction (Bertram and Schneekluth 1998), the hull efficiency is specified directly as 1.10 for hulls with $c_B < 0.7$ and 1.25 for hull with $c_B > 0.7$. This corresponds to the clusters seen in the results in Kristensen and Lützen (2012).
(6) A standard propeller series developed by the authors is used to create a propeller geometry
(7) The open-water propeller curves are estimated using the OpenProp software (Epps et al. 2009).
(8) Engine curves are derived from MAN (MAN 2017).
(9) A dynamic route simulation part is available in the model; however, it was not used in the current study.

To reduce the uncertainty of the prediction of the FC, improvements to the model presented in Tillig et al. (2017) were made in four areas: (i) the wetted surface prediction, (ii) resistance prediction, (iii) the prediction of the added resistance in waves and (iv) the prediction of the propulsive coefficients.

Concerning (i) and (ii), numerical standard hull series were developed by the authors. The numerical standard hull series are highly flexible parametric hull models that use only main dimensions as input, i.e. the length, the beam, the draft, the propeller diameter and the displacement. The models were developed using the CAESES software (Friendship-Systems 2017). At the time of the study, numerical standard series were available for slender hulls with wide sterns and a block coefficient between 0.55 and 0.7 and for full block ships with a block coefficient between 0.73 and 0.85. With these series at hand, hull forms for CFD and wetted surface computations are already available in the beginning of a design project. Wetted surface estimations are only used from the standard series, since this proved to give the most accurate approximation for a wide range of ship types.

To obtain higher robustness of the resistance, the effective wake and the added resistance in waves predictions, the average of several methods are used in these components, as given in the list above. Compared to the model in Tillig et al. (2017), the empirical resistance prediction method developed by Hollenbach (1998) and all three employed added resistance methods were added to the model. All of the three added resistance prediction methods, the STA2, the NTUA-SDL and the modified NTUA-SDL method, are empirical methods that aim to derive a transfer function for the added resistance in waves based on ship particulars. The ITTC spectrum (ITTC 2014b) is used in the prediction.

3. Method of uncertainty prediction of the fuel consumption

The uncertainty analysis was performed using the Monte Carlo method, which simulates 7–10 random variables, depending on the design phase. Results of a convergence test with 100,000 and 10,000 samples, showed a difference in total standard deviation as low as 0.0001. Following these results 10,000 samples were used in the study.

All identified random variables (see Equation (1)) are assumed to be normal distributed. For all variables, the mean value is represented as the value predicted by the ship energy systems model with the input available in the design phase in question; i.e. it differs between design phases. In this study, the mean values of the FC in phase I and phase II are identical because an adjustment would have been biased by the available model test results. The standard deviations are obtained by comparing different variants of hulls with the same predicted mean value, by comparing different methods or by specifying standard errors of the methods (i.e. model tests). During the simulation for design phase I, the propeller design is updated according to the predicted propeller loading. In design phases II–IV, the propeller remained unchanged for all variants. A summary of all random variables and their standard deviations as well as the results of the simulations are shown in Tables 3 and 4.

4. Method uncertainty

The definition of method uncertainty used in this study is the sum of uncertainties that are related to parameter uncertainty, structural uncertainty (i.e. model inadequacy), experimental uncertainty (observation error), and interpolation uncertainty. Following this definition, uncertainties related to model tests, empirical methods or numerical methods but not due to design/parameter/dimension assumptions are categorised as method uncertainties. If model test results are used, the measurement uncertainty for such test is used, while the spread of the results from different empirical methods is used to specify an uncertainty for the other components. The latter procedure requires that a set of validation data (e.g. model tests) is within the specified uncertainty of the predicted value.

4.1. Wetted surface

The wetted surface is obtained using the standard series hull and a numerical computation of the hull surface below the waterline. Any uncertainties due to the computation methods would be due to differences in numerical computation algorithms. Such differences are small and can be neglected for the purpose of the study. Thus, the method uncertainty for the wetted surface is zero.

4.2. Calm water resistance coefficient

The frictional part of the resistance is well described by the ITTC friction line (ITTC 1999). Thus, the unknown (random) variables are the viscous pressure and the residual resistance, which are denoted as $k * c_F$ and c_R, respectively, where k is the form factor. In Figure 2, the results of different methods to predict the viscous pressure and the residual resistance are shown for the two reference ships. Compared methods are the predicted value from the ship energy systems model, as discussed in Section 2, as well as the methods of Hollenbach (1998), Kristensen and Lützen (2012), Holltrop Mennen and the CFD computations using the numerical standard series hull. Model test results are shown for comparison. The standard deviation of the three methods used in the model (Hollenbach, Kristensen and Lützen and CFD) is shown as dark grey area around the predicted value (green line).

A good agreement of the predicted resistance and the model test can be observed, with the model test results being within the standard deviation of the three employed methods. With these results, it can be concluded that the method uncertainty of the resistance coefficients ($k * c_F + c_R$) prediction is well covered using the standard deviation of the three methods which are included in the energy systems model. With this approach, the uncertainty for the resistance coefficients varies between 5% and 20% for the RoRo ship and 3% and 20% for the tanker, respectively.

4.3. Effective wake

Figure 3 presents a comparison of the employed methods for effective wake prediction for the reference ships, with the results from model tests included for comparison purposes. The results show the model tests prediction close to the average value of the empirical methods and well within the standard deviation of the empirical methods. It can thus be assumed that the employed methods cover the span of possible predictions for a ship, and the standard deviation of all empirical formulae can be used as the standard deviation for the uncertainty prediction. This results in a larger standard deviation for the tanker (12%) compared to the RoRo ship (7%).

4.4. Hull efficiency

In Kristensen and Lützen (2012), the hull efficiency of a group of ships is shown. The values for the prediction in the energy systems model are fixed to 1.10 for slender hulls and 1.25 for higher block hulls, as discussed in Section 2. In the presented analysis in Kristensen and Lützen (2012), all ships had a hull efficiency between 1.00 and 1.40. For this study, the uncertainty must account for this spread. Thus, a standard deviation of 6% is defined for both slender and high-block ships. With this definition, the 95% confidence interval would be a hull efficiency of 0.97–1.23 for slender ships and 1.10–1.4 for high-block ships.

4.5. Propeller efficiency

In design phases I and II, propeller open-water characteristics are computed using the OpenProp software (Epps et al. 2009). The accuracy of this approach was investigated using six Wageningen B-series propellers (Lewis 1988). The published model test results were compared to the computed values obtained with OpenProp. The investigated propellers were 4-bladed propellers, with an area ratio of 0.55 and 0.85 and a design pitch (P/D) of 0.6, 0.8 and 1.0. In Figure 4, the results from the computations are presented as continuous lines, and the results from model tests are given as crosses. The standard deviation between the model test results and the computation is approximately 5% for the range of interest, i.e. advance ratios J between 1% and 65% below the advance ratio with maximum efficiency.

4.6. Added resistance in waves

In Liu and Papanikolaou (2016), the NTUA-SDL and the STAWAVE2 empirical methods are compared to model tests and a far-field method applied to seven ships in head seas between 1.5 and 5.5 m significant wave height. Five of the ships were

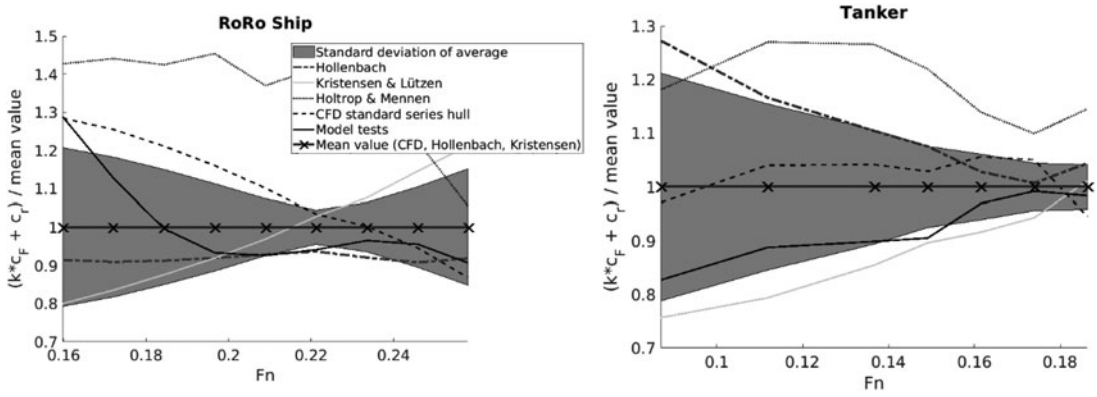

Figure 2. Viscous pressure and residual resistance according to different methods, relative to the mean value (predicted value from the energy systems model), for the RoRo ship (upper) and the tanker (lower).

series 60 hulls with different block coefficients; the others were more modern ships, a bulk carrier and a large container carrier (KVLCC). The results showed the good agreement of the two empirical methods, especially for the two more modern ships and seas up to 4 metres.

A similar comparison was performed using the software SHIPFLOW motions (Flowtech 2016) where the results are presented in Figure 5. The empirical methods agree well with the CFD computations in sea state 4 but show larger deviations in sea state 6. It must be noted that the computations were run in irregular head seas instead of several computations in regular seas to obtain the transfer function, which would be a better practice but more time-consuming.

In Nabergoj and Prpic-Orsic (2007), however, the comparison of five different semi-empirical methods showed a difference of up to 100% of the added resistance, especially in higher waves. This is three times as high as the mean absolute percentage error of the STAWAVE2 method compared to model tests on a diverse fleet of 50 vessels, as reported in Grin (2015). With these results, it must be concluded that it is still difficult to

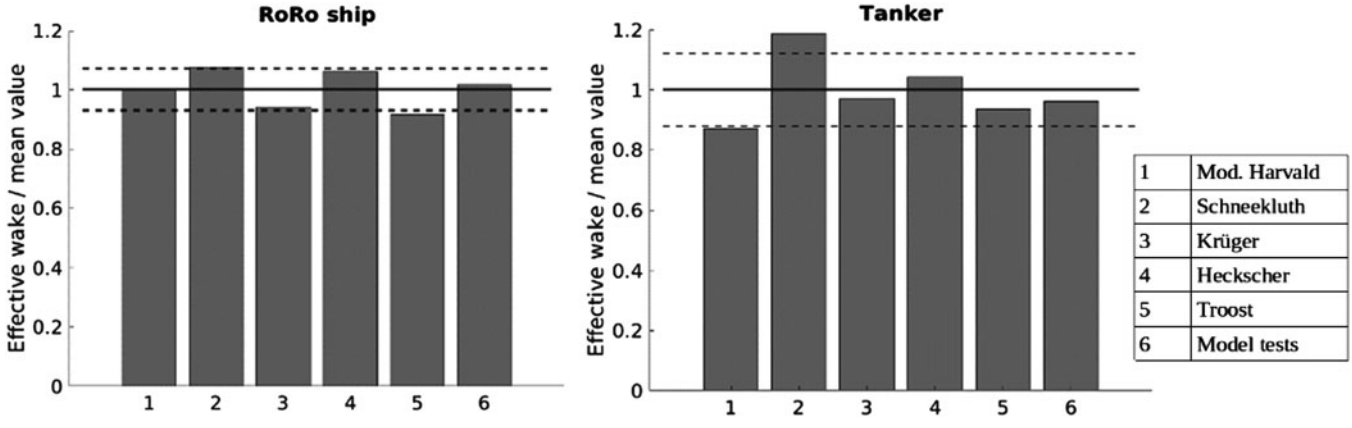

Figure 3. Comparison of wake prediction methods for the RoRo ship (left) and the tanker (right).

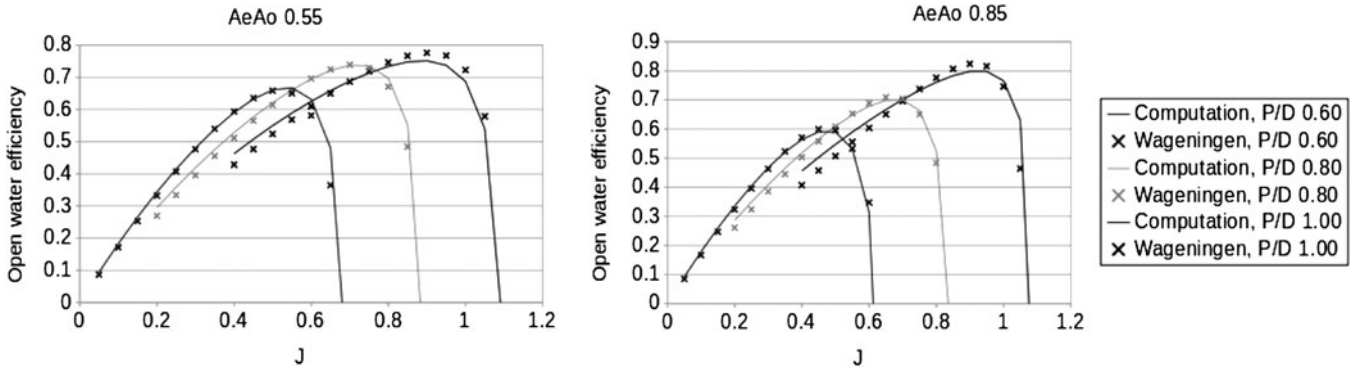

Figure 4. Comparison of OpenProp computations with model test results of Wageningen B-series propellers.

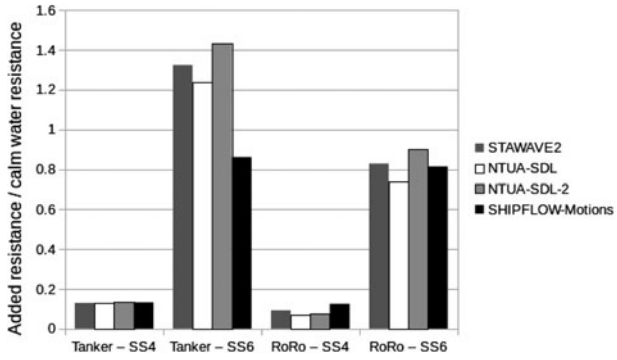

Figure 5. Comparison of added resistance in head seas for the RoRo ship and the tanker in two sea states (SS), using four different methods.

accurately predict the added resistance in waves using empirical and semi-empirical methods.

In the ship energy systems model, the average of the NTUA-SDL, STAWAVE2 and the improved NTUA-SDL method is used as the mean value of the added resistance in waves (see Section 2). The standard deviation among these three empirical methods is used as the standard deviation for the uncertainty analysis. For sea state 4, the standard deviation is computed to be 12.6% for the RoRo ship and 3.9% for the tanker.

4.7. Main engine SFOC

The prediction of the specific fuel oil consumption (SFOC) is based on the information provided by the engine manufacturer MAN (MAN 2017). According to MAN, the SFOC may vary within ±5%, which can be seen as the 95% confidence interval. With some margin for interpolation errors, the standard deviation for the SFOC can thus be defined to 3%.

4.8. Calm water model test results

The ITTC has presented several case studies on how the uncertainty of model test results can be estimated. The results from these studies showed the following (see ITTC 2014a,c,d):

(i) The standard deviation of the measured resistance was estimated to be 1%.
(ii) The standard deviation of the thrust deduction was estimated to be 5%.
(iii) The standard deviation of the effective wake was estimated to be 2%.
(iv) The standard deviation of K_T and K_Q was estimated to be 0.73% and 0.85%, respectively.

The above values are used for the uncertainty prediction. During model tests, form factors are typically rounded off to a precision of 0.005. With this in mind, a standard deviation of the form factor of 0.01, i.e. 5% for a form factor of 0.20, is reasonable. Note that the uncertainty of the form factor shall only include errors in the derivation of the form factor from the Prohaska plot, i.e. no measurement uncertainties.

4.9. Wind tunnel model tests

An uncertainty study of wind tunnel tests is reported in Yen and Bräuchle (2000). The 95% confidence interval for the drag coefficient is there estimated to be 4%. According to this, the standard deviation of the wind resistance coefficient can be defined to be 2%.

5. Design uncertainty

Design uncertainty is the parametric variability, which comes from the variability of input variables of the model. It will influence a ship's energy performance if there is a difference between the assumed design and the manufactured and delivered design. It could also be possible that details and design features are not accounted for correctly in the methods used in the ship performance simulations. The variations that are done to estimate the design uncertainty must thus be of a type that is not included in the methods used. The FC prediction shall be valid for a well-performing ship and the standard deviations are set to capture potentially better performing ships. Due to the assumed normal distribution, this procedure will neglect ships that perform worse with regard to FC. These ships might be outside of the 95% confidence interval of the prediction, but neither are they subject of the study since such ships must be seen as outdated due to their high FC.

5.1. Wetted surface

A numerical analysis of the wetted surface of 2500 hulls for each reference ship was performed based on the numerical standard series hulls. A list of the variables that were varied (upper/lower bounds) is presented in Appendix 1. The variables and their boundaries were selected in a way to produce varying geometries but stay within the limits of what typically is seen as a normal hull form for the ship type. With the standard hull series as a baseline (a value of 1), the relative variation of the wetted surface is presented in Figure 6. The standard deviation was calculated to be 1% for the RoRo ship and 0.8% for the tanker.

5.2. Resistance coefficients

The same hull variations that were used for the wetted surface study in Section 5.1 were used to investigate the variability of the viscous and residual resistance coefficients ($k * c_F + c_R$) due to changes of the hull form. All hull variants were analysed using potential and viscous computations with the SHIPFLOW software; see Appendix 1 for information about the parametric variation.

Figure 7 presents the results from the parametric variation; note that the resistance coefficients are calculated back to the mean wetted surface as

$$c_{\text{norm}} = c_{\text{computed}} \times S_w/\mu_{Sw}. \quad (3)$$

It should be emphasised that all hull forms were created randomly; thus, it is likely that lower performing hulls were created rather than good designs with regard to ship resistance performance.

In the standard deviation calculation, outliers were disregarded. An outlier was defined as a hull with a wave pattern resistance more than twice as high as the wave pattern resistance of the standard hull. The standard deviation of the remaining

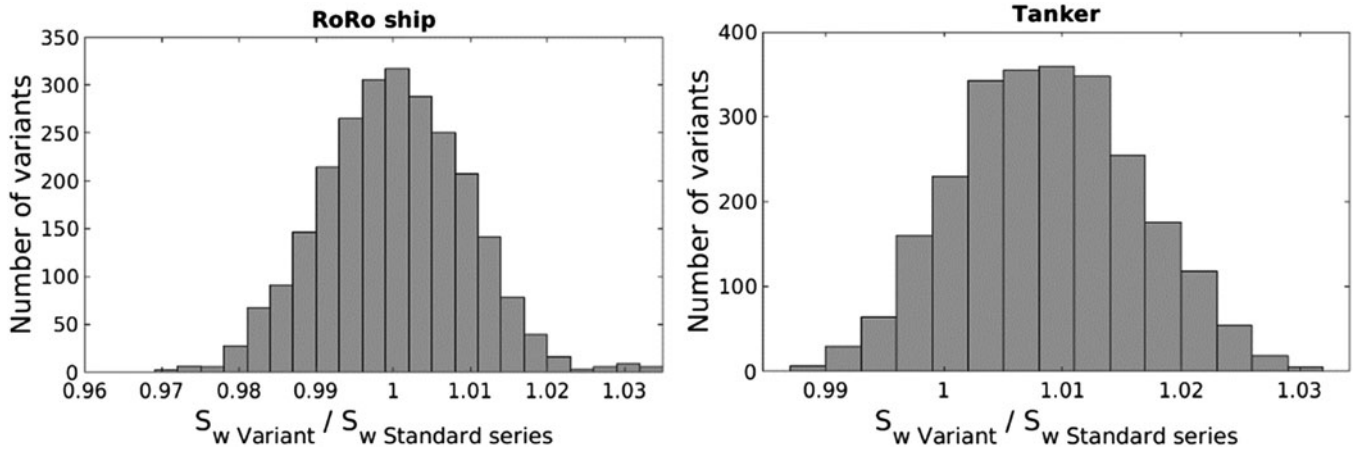

Figure 6. Histograms of the wetted surface variation due to hull form changes for the RoRo ship (left) and the tanker (right).

populations of hulls was computed to be 3.1% for the RoRo ship and 6.3% for the tanker.

5.3. Effective wake

In Section 5.2, only resistance computations were performed; thus, only the nominal wake is available for the hull variations. The computed standard deviation of the nominal wake was approximately 10% for both reference ships. In Kristensen and Lützen (2012), effective wake fractions from model tests are compared with a prediction according to Harvald. The entire fleet showed a scatter (maximum to minimum recorded) of the effective wake from model test of approximately 24%. With both the results from CFD and the results from model tests, 10% is selected as the standard deviation for the uncertainty analysis.

5.4. Propeller efficiency

In the ship energy systems model, a numerical propeller standard series similar to the Wageningen standard series is integrated. Propellers of the numerical standard series are adjusted to the required thrust of the hull and analysed using the OpenProp software. The design of these standard propellers was varied to obtain the variability of the propeller efficiency due to design changes. The design variables were the propeller diameter, the area ratio and the chord length distribution; see Appendix 2 for more information about the upper and lower boundaries. In total, 500 randomly created variants were investigated. In Figure 8, the results from the variation study are presented. The standard deviation due to design variations is computed to be 2%. Note that the propeller variants are randomly created; thus, propellers with better performance and characteristics can be achieved by optimisation.

5.5. Air/wind resistance

The mean value of the wind resistance is estimated using the coefficients presented in Blendermann (1994) and Blendermann (1993). In these studies, coefficients are presented for 15 different ship types from a total population of 24 ships. To compute a variability of the resistance coefficient due to different designs, a larger group of ships would be required. However, the standard deviation of the longitudinal force coefficient for all studied ships (of different types) was 10.5% (Blendermann 1993). All cargo ships, excluding tankers, which have a considerably higher coefficient, show a standard deviation of 5%. It is assumed that

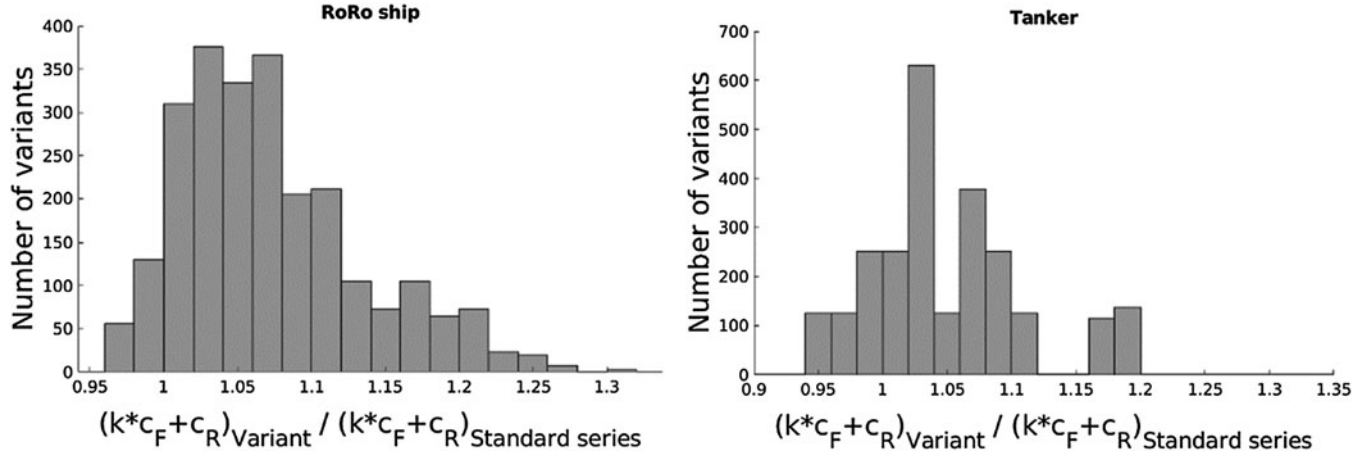

Figure 7. Histogram of the wave pattern and viscous resistance ($k * cF + cR$) relative to the standard series, for the RoRo ship (left) and the tanker (right).

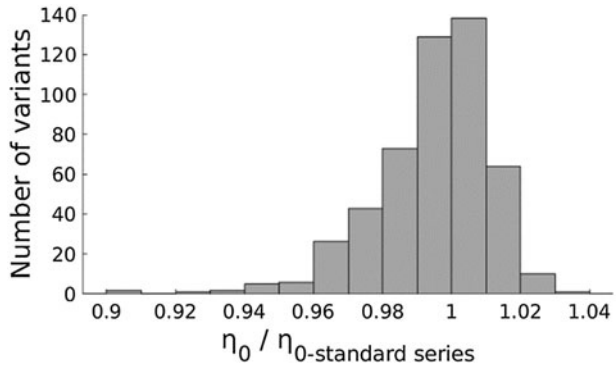

Figure 8. Histogram of the results of propeller design variation.

the standard deviation of the force coefficients of ships of the same type is lower, here set to 3%, which agrees with the standard deviations presented in Kristensen and Lützen (2012). Additionally, the transverse and longitudinal projected areas of the ships are subject to design variations. The projected areas are computed as follows:

$$\text{Transverse area}: A_T = B \times (D_h - T_m) + B_h \times h), \quad (4)$$

$$\text{Longitudinal area}: A_L = L_{oa} \times D_h + h \times L_h. \quad (5)$$

The depth D_h is estimated using the linear formula given by Bertram and Wobig (1999):

$$D_h = 0.087 \times L_{PP}. \quad (6)$$

The superstructure height h is based on the number of decks and a general deck height of 3 m, with 2 m added for equipment and funnels. The number of decks and the length of the superstructure (L_h) are set according to the ship type and size. For cargo ships, it can be assumed that the biggest expectable difference would be one deck more or less. The standard deviation of the transverse area is computed to 6% for the RoRo ship and 7% for the tanker. For the longitudinal area, the standard deviation is 3% for the RoRo ship and 1% for the tanker.

5.6. Added resistance in waves

Due to the high computational effort in calculating the added resistance in waves, only three hull form variants are studied: the hull form from the numerical standard series as a baseline, one hull designed for high added resistance, i.e. large bulb, large flare and blunt waterline, and a hull designed for small added resistance, i.e. small and slender bulb, small flare and slender waterline. Due to the low number of hull variants, the results should only be treated as a rough idea of the differences and not as a real variation study.

The difference in added resistance was 24% for the tanker and 4.5% for the RoRo ship. Since the hull variants were extreme designs, it is assumed that all hull designs will be within these ranges. The standard deviation is thus set to 6% for the tanker and 2% for the RoRo case.

6. Results

6.1. Results from the uncertainty analysis

Detailed results from the analyses and discussions presented in Sections 4 and 5, and the results of the Monte Carlo simulations are presented in Table 3 for the RoRo ship and in Table 4 for the tanker. The values are presented at the service speed, i.e. a Froude number of 0.19 for the RoRo ship and 0.16 for the tanker. The results from the Monte Carlo simulations are shown for the delivered power (P_D) and the fuel consumption (FC) in (i) calm water and no wind and (ii) sea conditions (head waves, sea state 4 and Beaufort 4 wind from ahead).

The largest reduction in uncertainty occurs when going from the design phase II to phase III. The reason is that model test results become available in phase III. The standard deviation of the FC at sea drops from approximately 9.5% to 4.3% for the RoRo ship and from 8.9% to 3.8% for the tanker. Concerning the uncertainties of the terms in Equation (1), the largest difference between these phases is found in the effective wake, with the standard deviation dropping from 7% (RoRo ship) and 12.1% (tanker) to 2%.

A comparison of the results between the RoRo ship and the tanker shows that the design uncertainties are larger for the tanker; see, for example, the difference in the total uncertainty between phase I and phase II. For both ships and in all design phases, the uncertainty of the FC is approximately 0.5%–1.5% higher than the uncertainty of the delivered power.

An illustration of the changes in mean value and the standard deviations of the FC at sea is shown in Figure 9 for the RoRo ship and Figure 10 for the tanker. The values shown are the changes to the mean value of phase IV:

$$\Delta\mu = \mu - \mu_{\text{phase IV}}. \quad (7)$$

According to Section 3, the mean value was not adjusted between phases I and II. For the RoRo ship, the results in Figure 9 show that the mean value in phases I and II is 5%–10% lower than the mean value in phases III and IV, with the biggest differences found at low speeds. It is found that the mean value from phases III and IV is within the standard deviation from the mean value of phases I and II. It can be identified that at low speeds, the empirically predicted resistance is considerably lower than the measured resistance in model tests. In addition, the measured hull efficiency and, especially, the propeller efficiency are lower than empirically predicted, with the latter being outside the defined uncertainty of the propeller efficiency. Finally, for the tanker, Figure 10 shows that the mean values of phases I and II are within the standard deviation of the mean value of phases III and IV, despite the larger assumed design uncertainties.

6.2. Ship operation case – comparison with full-scale measurements

The improved ship energy systems model was applied on a real ship operation case, for demonstration purposes. Measurement data from the performance monitoring system were available from several journeys for the RoRo reference ship. The environmental conditions and ship speeds from those journeys were used to predict the FC using the methods available in design

Table 3. Summary of standard deviations (relative to mean) for the RoRo case at $Fn = 0.19$, for calm water (*CW*) and operational condition (*sea*).

	Design stage							
	I		II		III		IV	
	D	M	D	M	D	M	D	M
S_W	1%	–	–	–	–	–	–	–
$k * c_F + c_R$	3.1%	6.4%	–	6.4%	–	4.1%	–	4.1%
w_e	10.0%	7.1%	–	7.1%	–	2.0%	–	2.0%
η_H	–	6.0%	–	6.0%	–	–	–	–
t	–	–	–	–	–	5.0%	–	5.0%
η_0	2.0%	1.5%	–	1.5%	–	1.2%	–	1.2%
A_T	6.0%	–	6.0%	–	6.0%	–	–	–
A_L	3.1%	–	3.1%	–	3.1%	–	–	–
c_X	3.0%	2.0%	3.0%	2.0%	3.0%	2.0%	–	2.0%
R_{AWaves}	2.2%	12.6%	–	12.6%	–	12.6%	–	12.6%
sfoc	–	3.0%	–	3.0%	–	3.0%	–	3.0%
$P_D(CW)$	10.0%		8.9%		2.1%		2.1%	
$FC(CW)$	10.4%		9.4%		3.7%		3.7%	
$P_D(sea)$	10.5%		9.0%		3.2%		3.2%	
$FC(sea)$	10.2%		9.5%		4.3%		4.2%	

phase I; i.e. real operational data are compared to a very early prediction of the performance. The results from a simulation of one journey are shown in Figure 11, which also presents the expected FC according to the uncertainty analysis, including the standard deviation. In Figure 12, the measured apparent wind speed and the predicted wave height are shown. By comparing these figures, it can be observed that in periods with low apparent wind and some waves, the predicted FC is, on average, approximately 5% lower than the measured value. This is similar to the results obtained from the comparison given in Section 6.1. Larger deviations are found with increasing apparent wind. In fact, the ship experiences a power increase due to the wind of about five times of the predicted power increase. Towards the end of the journey, the FC predicted by the simulation model is only approximately 60%–70% of the measured one. No apparent reason can be identified. Sea conditions were

Table 4. Summary of standard deviations (relative to mean) for the tanker case at $Fn = 0.16$, for calm water (*CW*) and operational condition (*sea*).

	Design stage							
	I		II		III		IV	
	D	M	D	M	D	M	D	M
S_W	0.8%	–	–	–	–	–	–	–
$k * c_F + c_R$	6.3%	6.0%	–	6.0%	–	2.5%	–	2.5%
w_e	10.0%	12.1%	–	12.1%	–	2.0%	–	2.0%
η_H	–	6.0%	–	6.0%	–	–	–	–
t	–	–	–	–	–	5.0%	–	5.0%
η_0	2.0%	1.5%	–	1.5%	–	1.2%	–	1.2%
A_T	7.0%	–	7.0%	–	7.0%	–	–	–
A_L	1.2%	–	1.2%	–	1.2%	–	–	–
c_X	3.0%	2.0%	3.0%	2.0%	3.0%	2.0%	–	2.0%
R_{AWaves}	6.1%	3.9%	–	3.9%	–	3.9%	–	3.9%
sfoc	–	3.0%	–	3.0%	–	3.0%	–	3.0%
$P_D(CW)$	13.7%		8.3%		2.3%		2.3%	
$FC(CW)$	13.8%		8.8%		3.8%		3.8%	
$P_D(sea)$	12.6%		8.4%		2.3%		2.3%	
$FC(sea)$	12.9%		8.9%		3.8%		3.8%	

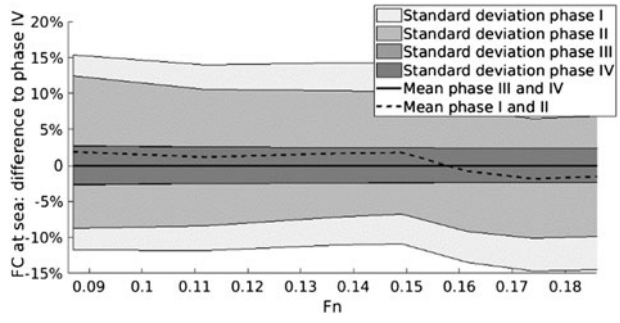

Figure 10. Differences in mean value and standard deviation of the fuel consumption at sea over the speed for the tanker.

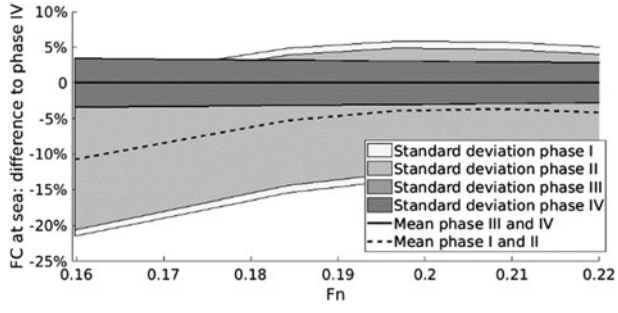

Figure 9. Differences in mean value and standard deviation of the fuel consumption at sea over the speed for the RoRo ship.

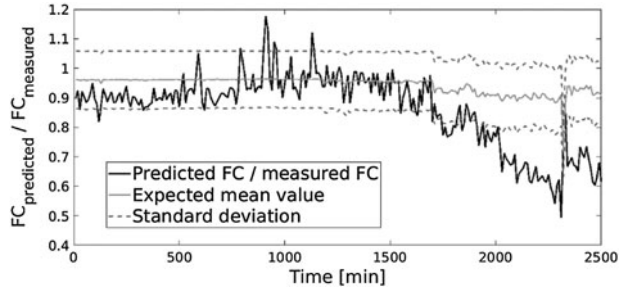

Figure 11. Relative fuel consumption for one journey of the RoRo ship.

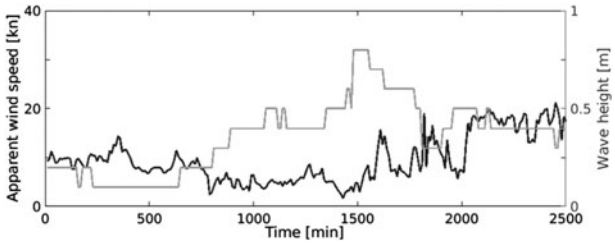

Figure 12. Environmental conditions during the journey.

calm with only approximately 20 knots of apparent wind and 0.5 metres of predicted wave height. It must be concluded that unknown factors cause a power increase or that the measurement error is large in this period. Some missing measurements are, e.g. the water depth, rudder angle and water current, especially the latter can cause huge deviations in the power-to-speed ratio.

6.3. Discussion

This study has shown that there is a clear trend in the reduction of uncertainties in the FC prediction when more information, appropriate models and methods are used throughout the ship design process. From the big difference between phase II and phase III, it can be concluded that the calm water power prediction introduces a large uncertainty. Further analysis shows that mainly the propulsive coefficients, especially the effective wake and hull efficiency, are problematic to predict in an early design phase. The empirical methods must be improved, e.g. by more standard series computations or tests. Consequently, the propulsive coefficients also cause the mean value of an early prediction to differ from the prediction obtained using model test results.

The propeller efficiency for the RoRo ship was lower compared to the model test results, which is unexpected after the analysis presented in Sections 3 and 4. The reference RoRo ship has a controllable pitch propeller with an ice class. Although the model should account for this, more analysis is required to investigate if and how the applied corrections could be improved.

The agreement of FC predictions throughout the design phases was much better for the tanker. This might indicate that the assumed design uncertainties are too high. However, in both cases, more statistics and more reference ships are needed before adjustments to the model can be made. Furthermore, the analysis was carried out in rather calm weather (sea state 4). It results in a low influence of the added wave resistance which is a source of large uncertainty. It can be assumed and expected that the uncertainties are higher for higher sea states until better methods are available for added resistance prediction. Finally, it was assumed that no model test results in waves were available in design phase IV. If this were the case, the total uncertainty would likely be even less.

7. Conclusions

The study presented an approach that can be employed for the prediction and uncertainty analysis of the FC of ships during the design process. A generic ship energy systems model was used in the calculations of the FC for one RoRo ship and one tanker. An important contribution from the study is the systematic overview and comparison of methods which are used in the ship energy systems model and a presentation how they are combined to increase the accuracy of the prediction and analysis of a ship's wetted surface, calm water resistance, effective wake, hull efficiency, air/wind resistance, propeller efficiency, added resistance in waves and main engine SFOC. The study presented a thorough analysis of how each module and its components influence the uncertainty of the entire generic ship energy systems model. Uncertainty was divided into two categories, design and method, to show how they are reduced from the early phases of a ship design process to the last phase when the ship's final design is known.

The uncertainty analysis of the FC, during operational conditions, and at the very early phase of the ship design process resulted in standard deviations of 10% and 13% for the RoRo and tanker vessels, respectively. At the final phase, when the ship design is finished and model test results are available, the standard deviations are reduced to less than 4% for both of the ships. This final phase represents the level of prediction accuracy typically available for a ship, which must be taken into account when potential energy saving measures are discussed or ships are compared. In reality, achievable savings and differences between ships of the same type are smaller than this uncertainty. Thus, special care must be taken in comparison studies, where it is advised to do direct comparison of the mean value prediction for different options, varying only the part affected by the measure, e.g. the resistance.

A comparison of the mean value of the predicted FC from the beginning of the design process and the finished design showed a difference of approximately 3% for the tanker and 6%–10% for the RoRo ship, depending on the ship speed. For the tanker, it was found that the mean value from phase I is within the standard deviation of the FC prediction obtained with all information and model tests available. For the RoRo ship, the deviation was larger due to large differences in the hull and propeller open-water efficiencies. More reference ships would be needed if the model should be adjusted. The empirical models must be further developed to capture the bulbous bow effects for ships experiencing this.

The ship energy systems model was applied on a real ship operation case with a RoRo ship for demonstration purposes. The predicted and measured FCs showed satisfactory agreement for parts of the journey and poor agreement for other parts. The predicted FC in the first half of the journey was, on average, 5% lower compared to the measured value, which agrees with the comparison of mean values from design phases I and IV. In the second part of the journey, larger deviations (up to 40%) appear, which cannot be explained with the data available and far exceed the expected deviation according to the present study. This deviation is most likely due to measurement uncertainties or environmental conditions that are not recorded. In order to enhance the ship energy systems model further, it is concluded that measurement uncertainties and errors during real ship operation conditions must be identified and possibly reduced to make full-scale measurements valuable for the validation of prediction models.

Acknowledgments

The project was funded by the Swedish Energy Agency by the contract no. 44454-1 for the project entitled "ShipCLEAN – Energy efficient marine transport through optimization of coupled transportation logistics and energy systems analyses". The project was also supported by Lighthouse (www.lighthouse.nu), a Swedish Maritime Competence Centre.

Disclosure statement

No potential conflict of interest was reported by the authors.

Funding

Energimyndigheten [grant number 44454-1].

Notes on contributors

Fabian Tillig holds the current position of a PhD student at Chalmers Technical University, Gothenburg, Sweden. He primarily works with energy systems modelling and the energy efficiency of ships. His previous experience includes jobs as a project manager and naval architect within model testing, hull design and CAE based hull improvement.

Jonas W. Ringsberg is a professor in Marine Structures at Chalmers Technical University, Gothenburg, Sweden, member of Royal Institution of Naval Architects (FRINA) and the Society of Naval Architects and Marine Engineers (SNAME). He is the chairman (2012–2018) of the International Ship and Offshore Structures Congress (ISSC) Technical Committee Quasi-static Response. His research interest and experience comprise energy systems modelling and the energy efficiency of ships, material mechanics, fatigue (HCF, LCF, fracture mechanics, multiaxial fatigue, residual stresses and welds), probabilistic methods and risk analysis, composite mechanics and materials, and Arctic engineering. Research activities are applied on collision and grounding, lightweight structures, fatigue of marine structures, dynamic response, ocean energy harvesting, risk analysis and risk assessment, Arctic engineering, and transport efficiency, safety and security.

Wengang Mao is an associate professor on the Department of Shipping and Marine Technology at Chalmers University of Technology, and a member of the International Ship and Offshore Structures Congress (ISSC) Committee Environment. His research activities have been devoted to the spatio-temporal modelling of sea environments and wave loads, ship structural fatigue and fracture, while currently more focus on weather routing development and better ship performance prediction through big data analytics.

Bengt Ramne, professor of the Practice at Chalmers University of Technology, MSc Naval Architect and Managing Director of ScandiNAOS AB. He has a broad experience in ship design, ship building and marine transportation systems. In the recent years he has acted as the technical coordinator in a number of successful project related to improved energy efficiency and implementation of alternative fuels in marine applications.

ORCID

Fabian Tillig http://orcid.org/0000-0002-9886-9147

References

Bertram V, Schneekluth H. 1998. Ship design for efficiency and economy. Oxford: Butterworth-Heinemann.

Bertram V, Wobig M. 1999. Simple empirical formulae to estimate main form parameter. Schiff Hafen. 11(1):118–121.

Blendermann W. 1993. Schiffsform und Windlast - Korrelations- und Regressionsanalyse von Windkanalmessungen am Modell [Shipshape and wind load- correlation and regression analysis of wind tunnel model tests]. Hamburg: Technische Universität Hamburg Harburg. Report No. 533.

Blendermann W. 1994. Parameter identification of wind loads on ships. J Wind Eng Ind Aerodyn. 51(1):339–351.

Calleya J, Pawling R, Greig A. 2015. Ship impact model for technical assessment and selection of Carbon dioxide Reducing Technologies (CRTs). Ocean Eng. 97(1):82–89.

Cichowicz J, Theotokatos G, Vassalos D. 2015. Dynamic energy modelling for ship-life-cycle performance assessment. Ocean Eng. 110(1):49–61.

Epps BP, Stanway MJ, Kimball RW. 2009. OpenProp: an open-source design tool for propellers and turbines. Proceedings of Propellers and Shafting 2009; Sept 15–16. Williamsburg (VA): Crown Plaza.

Flowtech. 2016. Shipflow user's manual, rev 6.2. Gothenburg: Flowtech AB.

Friendship-Systems. 2017. CAESES. [accessed 2017 May 15]. https://www.caeses.com/.

Grin R. 2015. On the prediction of wave-added resistance with empirical methods. J Ship Prod. 31(3):181–191.

Hollenbach KU. 1998. Estimating resistance and propulsion for single-screw and twin-screw ships. Ship Technol Res. 45(2):72–76.

ITTC. 1999. 1978 ITTC performance prediction method. ITTC-recommended procedures and guidelines. 7.5-02-03-01.4. http://ittc.info/media/1593/75-02-03-014.pdf.

ITTC. 2014a. Example for uncertainty analysis of resistance tests in towing tanks. 7.5-02-02-02.1, ITTC-recommended procedures and guidelines. http://ittc.info/media/4056/75-02-02-021.pdf.

ITTC. 2014b. Speed and power trials, Part 2, Analysis of speed/power trial data. ITTC-recommended procedures and guidelines. 7.5-04-01-01.2. Appendix D2. http://ittc.info/media/1936/75-04-01-012.pdf.

ITTC. 2014c. Uncertainty analysis, example for open water test. 7.5-02-02-02.1, ITTC-recommended procedures and guidelines. http://ittc.info/media/4076/75-02-03-022.pdf.

ITTC. 2014d. Uncertainty analysis, example for propulsion test. 7.5-02-03-01.2, ITTC-recommended procedures and guidelines. http://ittc.info/media/4064/75-02-03-012.pdf.

Kennedy MC, O'Hagan A. 2001. Bayesian calibration of computer models. J Roy Stat Soc B. 63(3):425–464.

Kristensen HO, Lützen M. 2012. Prediction of resistance and propulsion power of ships. Copenhagen: Technical University of Denmark. Project No. 2010-56, Report No. 04.

Leifsson L, Saevarsdottir H, Sigurdsson S, Vesteinsson A. 2008. Grey-box modeling of an ocean vessel for operational optimization. Simul Modell Pract Theory. 16(1):923–932.

Lewis E, editor. 1988. Principles of naval architecture. 3rd ed. Jersey City (NJ): Society of Naval Architects and Marine Engineers.

Liu S, Papanikolaou A. 2016. Fast approach to the estimation of the added resistance of ships. Ocean Eng. 112(1):211–225.

Liu S, Shang B, Papanikolaou A, Bolbot V. 2016. Improved formula for estimating added resistance of ships in engineering applications. J Mar Sci Appl. 15(1):442–451.

Lu R, Turan O, Boulougouris E, Banks C, Incecik A. 2015. A semi-empirical ship operational performance prediction model for voyage optimization towards efficient shipping. Ocean Eng. 110(1):18–28.

MAN. 2017. CEAS engine calculations. [accessed 2017 May 15]. http://marine.man.eu/two-stroke/ceas.

Nabergoj R, Prpic-Orsic J. 2007. A comparison of different methods for added resistance prediction. Presented at 22nd IWWWFB, Plitvice; Croatia.

Tillig F, Ringsberg JW, Mao W, Ramne B. 2017. A generic energy systems model for efficient ship design and operation. IMechE M J Eng Maritime Environ. 231(2):649–666. doi:10.1177/1475090216680672.

Vinther Hansen S. 2011. Performance monitoring of ships [dissertation]. Copenhagen: Technical University of Denmark.

Yen D, Bräuchle F. 2000. Calibration and uncertainty analysis for the UC Davis wind tunnel facility. Davis: University of California. Report. http://flight.engr.ucdavis.edu/wp-content/uploads/sites/33/2015/01/Calibration.pdf.

Appendices

Appendix 1. Variables during hull form variations.

Variable	Lower and upper bounds during variation	
	RoRo ship	Tanker
Bulb length coefficient	0.028–0.042	0.02–0.034
Bulb tip height coefficient	0.50–0.75	0.40–0.95
Change of waterline entrance angle (deg.)	−2.00 to 5.00	−15.00 to 15
Change of LCB (%)	−0.10 to 0.10	−0.10 to 0.10
Change of flat of side curve fullness	−0.20 to 0.20	–
Change of bulb area coefficient	−0.01 to 0.01	−0.025 to 0.025
Skeg sectional area centroid at boss (relative)	0.75–0.85	0.95–0.99
Skeg sectional area centroid at 40% aftbody (relative)	0.92–1.00	–
Skeg sectional area fullness at boss	0.40–0.60	0.50–0.75
Skeg sectional area fullness at 40% aftbody	0.40–0.60	0.50–0.70
Area factor of the sectional area curve for the skeg	0.90–0.96	0.80–0.95
Intersection curve (hull–skeg), start at bilge (relative)	–	0.40–0.60
Intersection curve (hull–skeg), horizontal fullness	–	1.00–1.10
Waterline fullness, forebody	–	0.63–0.70
Change of waterline area centroid, forebody	–	0–0.20
Bulbous bow sectional area curve area factor	–	1.05–1.15
Forebody sectional area curve, tangent at FP (relative)	–	0.75–0.95

Appendix 2. Variables during propeller design variations.

Variable	Mean	Max/Min
Diameter (m)	5.50	6.40/4.70
Area ratio	0.435	0.524/0.359
Change of chord length (%)	0	+7.2/−7.4
Change of profile thickness (%)	0	+4.2/−4.2